

The Permeability and Cytotoxicity of Insulin-Mimetic Vanadium Compounds

Xiao-Gai Yang,¹ Xiao-Da Yang,^{1,4} Lan Yuan,² Kui Wang,¹ and Debbie C. Crans³

Received November 20, 2003; accepted March 3, 2004

Purpose. The aim of this study was to investigate the mechanism of permeation and cytotoxicity of vanadium compounds, [VO(acac)₂], [VO(ma)₂], and vanadate.

Methods. Absorptive transport were carried out in Caco-2 monolayers grown on transwell inserts. Vanadium was quantified using inductively coupled plasma atomic emission spectrometry (ICP-AES). The change of Caco-2 cells in the microvilli morphology and F-actin structure was visualized by transmission electron microscopy and confocal laser scanning microscopy.

Results. The three vanadium compounds were taken up by Caco-2 cells via simple passive diffusion. [VO(acac)₂] were mainly transcellularly transported and exhibited the highest apparent permeability coefficients ($8.2 \times 10^{-6} \text{ cm}^{-1}$). The cell accumulation of [VO(acac)₂] was found to be greater than that of [VO(ma)₂], and vanadate caused much less accumulation than the other two compounds. Vanadium compounds induced intracellular reactive oxygen species, reduced the transepithelial electric resistance, caused morphological change in microvilli, and led to different perturbation of F-actin structure.

Conclusions. The three compounds exhibited different permeability due to different diffusion process and cellular uptake. The toxicity of vanadium complexes on Caco-2 monolayer involved F-actin-related change of tight junction and impairment of microvilli. The toxicity was also related to elevated intracellular reactive oxygen species (ROS) and their cellular accumulation.

KEY WORDS: Caco-2 cells; confocal laser scanning microscopy; cytotoxicity; F-actin; vanadium compounds.

INTRODUCTION

Based on their insulin-like action, a variety of vanadium compounds have been studied as drug candidates for diabe-

tes. Although some compounds are in clinical trial and encouraging results have been obtained, their clinical application is limited by two major problems (1–3): poor absorption from the gastrointestinal (GI) tract into the bloodstream and the gastrointestinal stress, the principle sign of vanadium toxicity. Therefore, current research on vanadium antidiabetic agents has focused on new organic coordination compounds with higher lipophilicity to improve absorption and lessen the GI irritation. Among the orally effective hypoglycemic vanadium entities such as peroxovanadium and organic-liganded vanadium complexes, large differences in therapeutic efficacy were observed (4,5). It has been proposed that biopotency is not only determined by a compound's activity, but also by the absorption, distribution, metabolism, elimination, and toxicity (ADME/T) properties (6,7); while the intestinal absorption is one major factor determining the bioavailability of an orally administered drug. Previously, we have used human erythrocytes as a model system to compare the transport of vanadium compounds and the interaction with the erythrocyte membrane (6) to pursue the factors that determine the biopotency of the vanadium compounds. However, the relationship between the chemical properties and their pharmacological effects or toxicity is still not clear. In many aspects, the human erythrocyte model does not resemble the gastrointestinal barrier, and the transmembrane transport does not resemble the absorptive transport. The fully differentiated Caco-2 cell monolayer represents a well-established model for the study of transport and mucosal toxicity of xenobiotics as well as a good alternative for *in vivo* studies (8,9). However, studies have been done only with undifferentiated Caco-2 cells, and the results showed that neither complexation nor oxidation state of vanadium alone were adequate predictors of relative absorption (10).

To investigate the factors leading to the different bioavailability of vanadium compounds and their relation to the cytotoxicity, the mechanism of permeation and effects on Caco-2 and the cell monolayer were studied with three vanadium compounds, including: (i) vanadate, a well-known inhibitor of phosphotyrosine phosphates and consequent stimulation of protein tyrosine kinases to activate the insulin receptor tyrosine phosphorylation (11); (ii) bis(maltolato)oxovanadium ([VO(ma)₂]), a "benchmark" compound with more effective insulin mimic activity than simple vanadium salt (12,13); and (iii) vanadyl acetylacetonate ([VO(acac)₂]), rated as a related effective agent in controlling hyperglycemia (14). Although the relative therapeutic efficacy of [VO(acac)₂] and [VO(ma)₂] is still in dispute (13,14), [VO(acac)₂] clearly has better hydrolytic and redox stability (5,6,15). Our results suggest that the activity of vanadium compounds might be complicated by their ADME/T properties.

MATERIALS AND METHODS

Caco-2 cells were obtained from American Type Culture Collection (Rockville, MD, USA). Fetal calf serum, Hanks' Balanced Salt Solution (HBSS), Earlier's Balanced Salts Solution (EBSS) and other culture media and supplements were obtained from Gibco (Grand Island, NY). Transwells were purchased from Corning Costar (Cambridge, MA, USA). 3-(4,5-dimethylthiazoyl-2-yl) 2,5-diphenyltetrazolium bromide (MTT), *N*-2-hydroxy-ethylpiperazine-*N'*-2-ethanesul-

¹ Department of Chemical Biology, School of Pharmaceutical Sciences, Peking University, Beijing 100083, China.

² Analytical Center of Peking University, Beijing 100083, China.

³ Department of Chemistry, and Cell and Molecular Biology Program, College of Natural Sciences, Colorado State University, Fort Collins, Colorado 80523-1872, USA.

⁴ To whom correspondence should be addressed. (e-mail: xyang@bjmu.edu.cn)

ABBREVIATIONS: AP, apical side; BL, basolateral side; Buffer H, HEPES-buffered isotonic solution; DCFH-DA, 2', 7'-dichlorofluorescein diacetate; DE, dihydroethidium; DIDS, 4,4'-diisothiocyano-2,2'-stilbene disulfonate; EBSS, Earlier's balanced salt solution; HBSS, Hanks' balanced salt solution; HEPES, *N*-2-hydroxyethylpiperazine-*N'*-2-ethanesulfonic acid; IC₅₀, 50% inhibition concentrations; ICP-AES, inductively coupled plasma atomic emission spectrometry; LSCM, fluorescence staining and laser scanning confocal microscopy; MTT, 3-(4, 5-dimethylthiazoyl-2-yl) 2,5-diphenyltetrazolium bromide; ROS, reactive oxygen species; TEER, transepithelial electrical resistance; [VO(acac)₂], canadyl acetylacetonate; [VO(ma)₂], bis(maltolato)oxovanadium.

fonic acid (HEPES), and 4,4'-diisothiocyano-2,2'-stilbene disulphonate (DIDS) were from Sigma (St. Louis, MO, USA). Dihydroethidium (HE) 2',7'-dichlorofluorescein diacetate (DCFH-DA), Hoechst 33258, and rhodamine-phalloidin were from Molecular Probes (Eugene, OR, USA).

Stock solutions of sodium metavanadate, $[\text{VO}(\text{acac})_2]$ and $[\text{VO}(\text{ma})_2]$ were prepared in HEPES-buffered isotonic solution (Buffer H) (NaCl, 135 mM; HEPES, 15 mM; pH 7.4). DCFH-DA and HE solutions were both prepared by dissolving in DMSO and diluting with Buffer H to final concentration of 5 and 5 μM , respectively.

Cell Culture

Caco-2 cells were cultured in Dulbecco's Modified Eagle's Medium (DMEM) containing 4.5 $\text{g}\cdot\text{L}^{-1}$ D-glucose, 3.7 $\text{g}\cdot\text{L}^{-1}$ NaHCO_3 , supplemented with 10% fetal calf serum, 1% nonessential amino acids, 100 $\text{U}\cdot\text{ml}^{-1}$ penicillin, and 100 $\mu\text{g}\cdot\text{ml}^{-1}$ streptomycin. The cells were incubated at 37°C in a humidified atmosphere of 5% CO_2 . All cells used in this study were between passages 40 and 60.

Permeation of Vanadium Compounds Across Caco-2 Monolayers

Caco-2 cells were seeded at a density of about 1×10^5 cells/ cm^2 on a Transwell insert filter (surface area = 1.1 cm^2 , pore size = 3 μm). Cells were left to grow for 21 days to reach confluence and differentiation. The transepithelial electrical resistance (TEER) of the monolayer was measured with a Millicell electrode resistance system (Millipore Corporation, Bedford, MA, USA), and TEER values of $>600 \Omega\cdot\text{cm}^2$ were routinely observed. The monolayers were washed twice with HBSS, and then 0–0.60 mM of the vanadium compounds ($[\text{VO}(\text{acac})_2]$, $[\text{VO}(\text{ma})_2]$, and vanadate) were added to either the apical side (vanadium dissolved in EBSS, pH 6.0) or the basolateral side (vanadium dissolved in HBSS, pH 7.4). HBSS solutions were added to the basolateral side. Then, the samples were shaken (37°C, 50 rpm) and 100 μl aliquots were taken from the receiver side at desired time intervals of 0–1 h.

To measure the amount of cell accumulation, the Caco-2 cells were washed three times after the above transport studies with 1 ml of ice-cold HBSS and 5 mM EDTA (pH 7.2) to remove residual medium and surface-bound metal ions. Then, the cells were collected and completely digested with 0.5 ml ultrapure nitric acid. The amounts of vanadium in the collected samples above were determined with inductively coupled plasma atomic emission spectrometry (ICP-AES) (Leeman Labs Inc., Hudson, NH, USA).

To investigate the effect of DIDS, the anion channel blocker, Caco-2 cells were preincubated with 0.1 mM of DIDS in EBSS for 30 min at 37°C. Then 5×10^{-4} M of each vanadium compound was added, and the transport experiments were carried out as described above. The effect of DIDS on tight junction and integrity of the monolayer was investigated by monitoring TEER values.

The apparent permeability coefficient across the Caco-2 cell monolayers (P_{app}) was calculated with the following equation:

$$P_{\text{app}} = (dQ/dt)/(A \cdot C_0)$$

Where dQ/dt is the flux of drug across the monolayer (mol

transported/s), A (cm^2) is the surface area of the inserts, and C_0 (M) is the initial drug concentration in the donor compartment.

Cytotoxicity Assay

The cells were seeded in 96-well microplates at 5000 cells/well and left in culture for 48 h. Then, the cells were incubated with various concentrations of vanadium compounds from 0 to 1.5 mM in 100 μl DMEM for 24 h. Afterwards, the medium was removed, and 100 μl MTT (5 mg/ml in phosphate buffered saline) was added to each well and kept for 4 h. The MTT medium was subsequently removed, and the formazan crystals were dissolved in 200 μl DMSO. The absorbance at 570 nm was measured 15 min later on a plate reader (TECAN SUNRISE, Mannedorf, Switzerland). Fifty percent inhibition concentrations (IC_{50}) was calculated by plotting the cell viability vs. vanadium concentrations and fitted to the Hill model using a MicroCal Origin program (Origin Lab Corporation, Northampton, MA, USA).

Cellular Superoxide ($\cdot\text{O}_2^-$) and H_2O_2 Assay

The cells were seeded in 6-well plates and cultured until 80–90% confluent and then treated with vanadium compounds (5×10^{-4} M) for 4 h. A fluorescence dye, HE or DCFH-DA, was applied to the cells after two washes and incubated for 20 min at 37°C. The cells were washed twice again with Buffer H and harvested for analysis on a flow cytometer with excitation at 488 nm and emission at 530 nm for DCFH-DA (FL-1 channel detector) or emission at 580 nm for HE (FL-2 channel). The samples were also observed under a laser scanning confocal microscopy (Leica TCS NT, Heidelberg, Germany).

Determination of Cell Monolayer Integrity

The Caco-2 monolayer was incubated with 0–1.0 mM of vanadium compounds in EBSS on the apical side for 60 min at 37°C. Then, the samples were shaken at 50 rpm. The integrity of the monolayer was monitored by measuring the transepithelial electrical resistance (TEER) using a Millicell electrode resistance system (epithelial voltohmmeter (World Precision Instrument, Sarasota, FL, USA).

Caco-2 Cell Morphology by Transmission Electron Microscopy

Caco-2 cells seeded on transwells were cultured for about 3 weeks. Transmission electron microscopic studies were performed on the Caco-2 cell monolayer exposed to the vanadium compounds on the apical side for 60 min and 120 min at 37°C. After wash of the cells with Buffer H, the polycarbonate membranes were cut and fixed with glutaraldehyde. Then, the samples were immersed consecutively in 1% osmium tetroxide and 1% uranyl acetate, dehydrated, and embedded in Epon. The thin sections, stained with uranyl acetate, were examined with a Hitachi 7100 electron microscope (Hitachi, Japan).

Fluorescence Staining of F-actin

Caco-2 cells seeded on the Petri dish for about 3 weeks were rinsed with HBSS and incubated for 1 h at 37°C in the presence and the absence of the vanadium compounds. The

cell monolayers were rinsed twice with HBSS and then stained with Hoechst 33258 (1 $\mu\text{g/ml}$) for 30 min at 37°C. After rinsing with HBSS, the cell monolayers were fixed with 3.7% formaldehyde solution and stained for 20 min with rhodamine-labeled phalloidin. The stained cells were washed several times with HBSS and were observed under laser scanning confocal microscopy. Fluorescence images were collected at 512 \times 512 pixels resolution with excitation at 567 nm (for rhodamine-labeled phalloidin-F-actin) and 363 nm (for Hoechst 33258).

RESULTS

The apparent permeability coefficients P_{app} , the bi-directional transport between apical and basolateral side, and the intracellular accumulation of the three vanadium compounds are shown in Table I and Figs. 1a–1c. The $[\text{VO}(\text{acac})_2]$ exhibited better permeability with P_{app} in the AP to BL direction at $8.2 \times 10^{-6} \text{ cm}^{-1}$, which is about 6–8-fold of that of $[\text{VO}(\text{ma})_2]$ ($1.46 \times 10^{-6} \text{ cm}^{-1}$) or vanadate ($1.04 \times 10^{-6} \text{ cm}^{-1}$). Because high rate of cell accumulation was observed for the three compounds (Fig. 1b) [about 25%, 10%, and 2% for $\text{VO}(\text{aca})_2$, $\text{VO}(\text{ma})_2$, and NaVO_3 , respectively], the real P_{app} values were expected to be higher. Nevertheless, the recovery of the transportation assays were found to be ~95% (taking into account the amount of the cell accumulation). $[\text{VO}(\text{acac})_2]$ and $[\text{VO}(\text{ma})_2]$ exhibited higher cell accumulation capacity, much more than that of vanadate; however, permeability of $[\text{VO}(\text{ma})_2]$ was about the same as vanadate.

As in Fig. 1(a), the rates of membrane permeation of the three vanadium compounds increased linearly with the concentration up to an upper range of the concentration tested (0.6 mM). The P_{app} constants for the three compounds were found to be concentration independent (Fig. 1c). The permeability of all the three vanadium compounds in the apical to basolateral ($P_{\text{app, A to B}}$) was about twice that of the basolateral to apical directions ($P_{\text{app, B to A}}$). As shown in Table II, DIDS had little effect on transport of the vanadium compounds.

Figure 2 shows the results of general cytotoxicity of the vanadium compounds measured by decrease of cell viability using the MTT assay (16). The IC_{50} values were calculated to be $0.80 \pm 0.16 \text{ mM}$ for $[\text{VO}(\text{acac})_2]$, $1.27 \pm 0.28 \text{ mM}$ for vanadate, and $1.78 \pm 0.26 \text{ mM}$ for $[\text{VO}(\text{ma})_2]$.

The effects of vanadium compounds on cellular ROS level in Caco-2 cells were analyzed by fluorescent staining of intracellular $\cdot\text{O}_2^-$ and H_2O_2 with HE (specific for $\cdot\text{O}_2^-$) and DCFH-DA (specific for H_2O_2) as described above. Both $\cdot\text{O}_2^-$

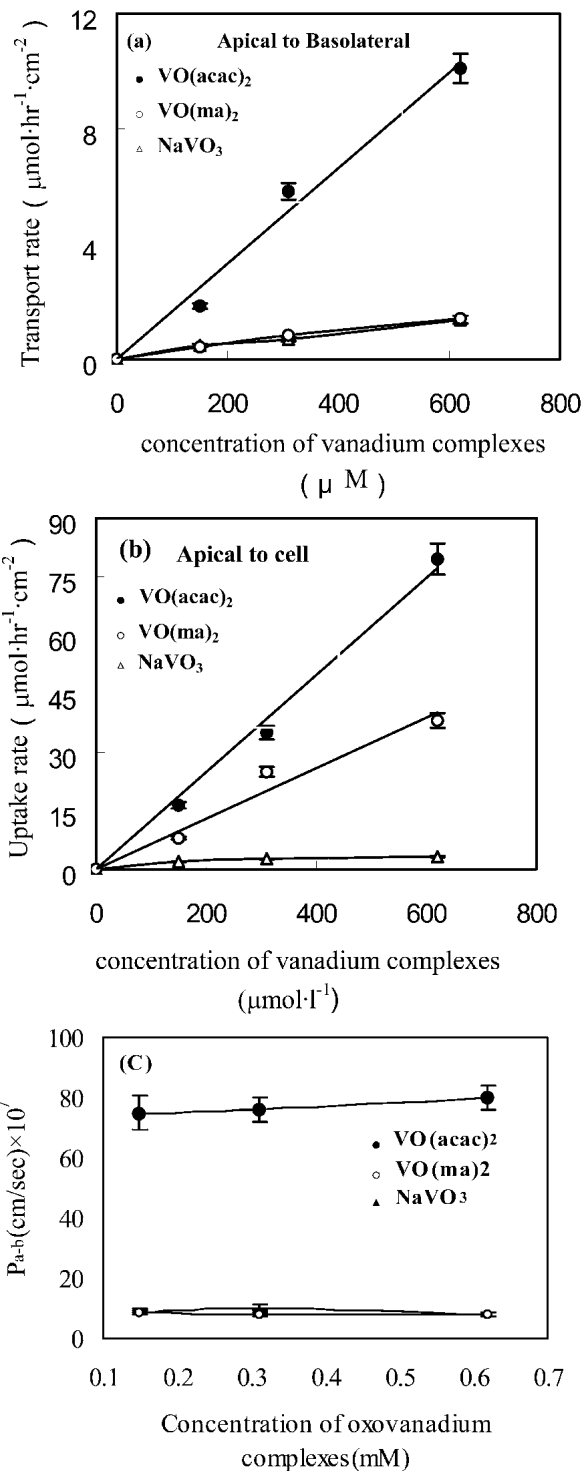


Fig. 1. Transport and cell accumulation of vanadium complexes in Caco-2 cells. (a) Plots of transport rate of vanadium compounds from apical to basolateral vs. the concentration, (b) plots of cellular uptake of vanadium compounds from apical side vs. the concentration, (c) plot of $P_{\text{app, A to B}}$ of vanadium compounds vs. the concentration. $[\text{VO}(\text{ma})_2]$ curve overlap with that of NaVO_3 . All data presented are means \pm SD of three measurements.

and H_2O_2 level were dramatically elevated in the presence of vanadium compounds (Figs. 3 and 4). The capacity of vanadium compounds to induce ROS was in the order $[\text{VO}(\text{acac})_2] > [\text{VO}(\text{ma})_2] \approx$ vanadate. Interestingly, the $\cdot\text{O}_2^-$

Table I. The Apparent Permeability Coefficients of Vanadium Compounds

Samples	$P_{\text{app}} \times 10^7$ ($\text{cm}^2/\text{s})^a$	
	A \rightarrow B ($P_{\text{app, a-b}}$)	B \rightarrow A ($P_{\text{app, b-a}}$)
NaVO_3	10.4 ± 1.2	5.5 ± 0.4
$[\text{VO}(\text{ma})_2]$	14.6 ± 0.7^b	6.7 ± 0.5^b
$[\text{VO}(\text{acac})_2]$	82.0 ± 6.7^b	41.0 ± 4.0^b

^a Each data point was the average of three assays.

^b Data was from Yang *et al.* (26).

Table II. Effects of DIDS on Vanadium Compounds Transport in Apical to Basolateral Direction

	$P_{app} \times 10^7$ (cm/s)		
	[VO(acac) ₂]	[VO(ma) ₂]	NaVO ₃
Control (- DIDS)	85.9 ± 11.1	10.8 ± 1.2	8.67 ± 0.64
+ DIDS (0.1 mM) ^b	83.1 ± 6.1	8.9 ± 0.97	7.64 ± 0.51

DIDS, 4,4'-diisothiocyano-2,2'-stilbene disulfonate.

^a Values are means ± SE; n = 3.

^b Caco-2 cells were preincubated with DIDS (0.1 mM) in the apical side for 30 min. Then, 6.0×10^{-4} M vanadium compounds in EBSS (pH = 6.5) in the presence of 0.1 mM of DIDS were added, and the amounts of vanadium in the basolateral side were measured after incubation for 60 min.

species was shown to locate in a specific area of the cytoplasm appearing as bright-color dots, whereas H₂O₂ was evenly spread within the cell.

The integrity of the Caco-2 cell monolayer was investigated by TEER measurement. The results showed that the TEER of monolayer decreased at the concentration of 1.0 mM (Fig. 5). The capacities of reducing TEER for the three vanadium compounds were [VO(acac)₂] (48% reduction) > [VO(ma)₂] (20% reduction) ≈ vanadate (16% reduction).

As shown in Fig. 6, the control Caco-2 cells had well-differentiated columnar shape with apical intact microvilli and tight junctions (Fig. 6a). Upon incubation with vanadium compounds for 1 h, microvilli lost regular organization and were no longer perpendicular to cell membrane. Numerous vacuoles appeared in the cytoplasm; however, the cells still exhibited an intact tight junction (Fig. 6b).

Figure 7 shows the fifth section of monolayer cells at a series of horizontal 1.1 μm optical sections of confocal images from apical to basolateral side. Compared with the control, [VO(acac)₂]-treated monolayer displayed condensation of F-actin at the periphery of the cells, whose nuclei also demon-

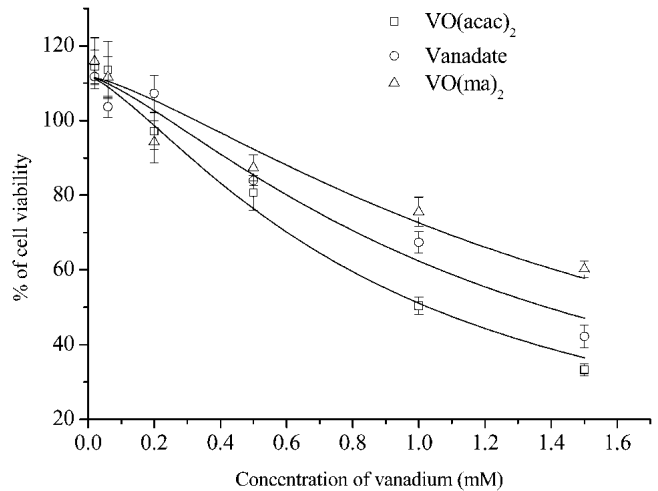


Fig. 2. Activity of mitochondrial dehydrogenase (MTT assay) after incubation with different concentrations of vanadium compound for 18 h. Data from six replicates are expressed as means ± SD.

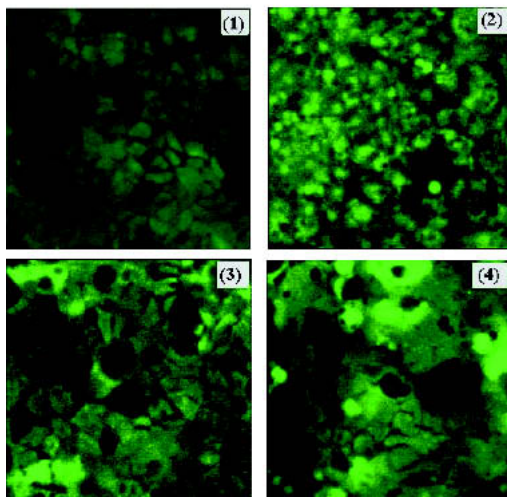
strated condensation. Treatment of monolayers with [VO(ma)₂] and NaVO₃ resulted in brighter signal of F-actin structure at the cell-cell contacts.

DISCUSSION

The experimental results indicate that all the three vanadium compounds pass through Caco-2 cell monolayer via the simple passive diffusion. Evidence includes:

(i) The rates of the three vanadium compounds increased linearly with the concentration and did not show saturation up to 0.6 mM (Figs. 1a and 1b), indicating that this permeation process is driven by the concentration gradient. It has been shown in previous studies with erythrocytes (6) that [VO(acac)₂] and [VO(ma)₂] were taken mainly by simple passive diffusion in the intact forms.

(A) H₂O₂ level



(B) ·O₂⁻ level

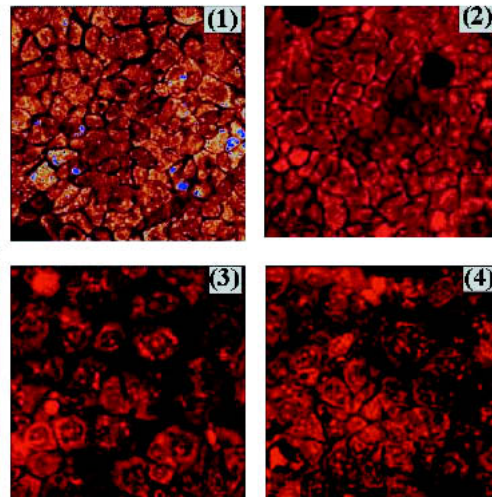


Fig. 3. The images of ·O₂⁻ and H₂O₂ generated inside the Caco-2 cells under a confocal microscope. ·O₂⁻ and H₂O₂ were stained by HE (red) and DCFH-DA (green), respectively, by incubation of the cells with 5 μM of the fluorescent dyes for 15 min at 37°C. (1) control, (2) [VO(acac)₂], (3) [VO(ma)₂], and (4) NaVO₃.

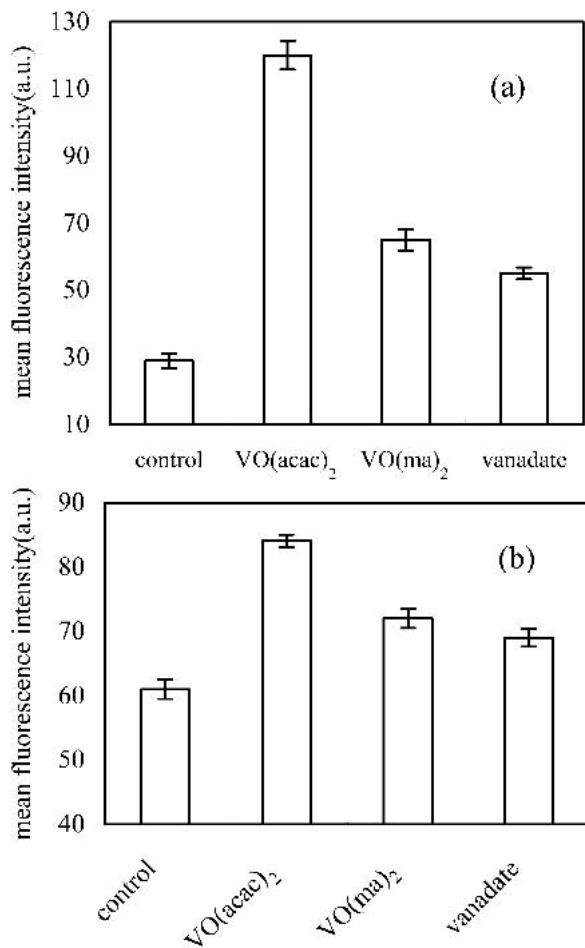


Fig. 4. Quantitation of (a) $\cdot\text{O}_2^-$ and (b) H_2O_2 in Caco-2 cells by HE and DCFH-DA fluorescent staining.

(ii) The fact that the P_{app} was independent of vanadium concentration (Fig. 1c) did not support involvement of an active transport mechanism.

(iii) No efflux was observed for any of the three compounds. The AP to BL permeability, as shown in Table I, is larger than the reversed direction. A ratio of ~ 2 for A to B permeability over that of B to A is unexpected for the simple diffusion process. The reasons might be (a) the 12-well transwell is not an equal volume system; the size of B side is 3-fold greater than A side. Transport of substance from A to B will generate higher concentration gradient than from B to A side after the transport process starts. Therefore, for passive diffusion, the P_{app} obtained from A to B is always larger than from B to A. (b) We have seen a significant cell accumulation of vanadium compounds. Binding of vanadium to biological macromolecules is expected during transmembrane permeation. The effects of vanadium on F-actin (see below) suggest that the cytoskeletal protein may be a major binding site for vanadium. Because the differentiated Caco-2 cells are polarized, the microvilli membrane side has a relatively larger surface and thus possesses a much higher binding capacity than the basolateral membrane side. When B to A transport is carried out, more binding of vanadium complexes to the microvilli membrane could result in less vanadium permeation across monolayer than that in the reverse transport direction.

(iv) The three compounds did not adopt the anion transport system because DIDS had little effect on transport (Table II). DIDS was shown to be a relatively specific anion carrier/channel inhibitor without significant change of the permeation properties of the monolayer (17,18). This situation is different with erythrocytes (6), where vanadate and oxidized species of $[\text{VO}(\text{acac})_2]$ and $[\text{VO}(\text{ma})_2]$ were shown to enter erythrocytes effectively via anion channel, and the transport of these compounds were eliminated by DIDS (6).

In addition, the results suggest that $[\text{VO}(\text{acac})_2]$ may primarily transport via transcellular pathway (passive diffusion through cytoplasm). For $[\text{VO}(\text{ma})_2]$ and vanadate, due to the very low P_{app} , paracellular pathway (passive diffusion occurring between cell junctions) may also contribute to the permeation process. It is also conceivable that much lower cellular uptake of vanadate should account for its very low membrane permeability.

The experimental results above suggested that simple diffusion could be the major pathway for both inorganic and organic vanadium compounds in oral administration. It is widely accepted that lipophilic drugs have better cellular permeability and absorption profiles than hydrophilic drugs. Therefore, lipophilicity could be one of the major determining factors for the oral bioavailability of vanadium compounds.

There is great difference in permeability between $[\text{VO}(\text{acac})_2]$ and $[\text{VO}(\text{ma})_2]$. This difference may partially account for the difference in biopotency between $[\text{VO}(\text{acac})_2]$ and $[\text{VO}(\text{ma})_2]$ (13,14). $[\text{VO}(\text{ma})_2]$ and $[\text{VO}(\text{acac})_2]$ are both vanadium(IV) coordination complexes formed from bidentate ligands and thus have many chemical similarities including their high lipophilicity. In erythrocytes, the two compounds exhibited almost the same capacity for cellular uptake; in Caco-2 cells, their capacities of cellular accumulation were shown to be close (Fig. 1b). However, $[\text{VO}(\text{ma})_2]$, shown by Caravan *et al.* (19), is less stable in aqueous solution and slowly oxidized by molecular oxygen to $[\text{VO}_2(\text{ma})_2]^-$ and

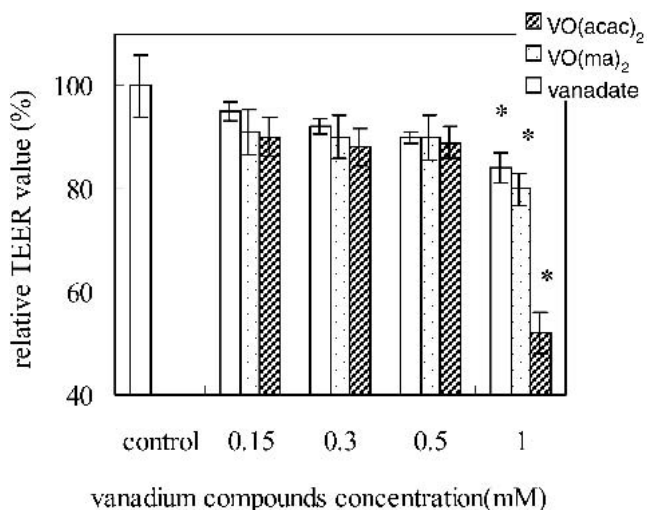


Fig. 5. Effect of $[\text{VO}(\text{acac})_2]$, $[\text{VO}(\text{ma})_2]$, and vanadate on TEER values of Caco-2 cell monolayer upon apical incubation. TEER values were obtained immediately after treatment with vanadium complexes for 60 min. Data are average of triplicate measurements. *Significantly different at $p < 0.05$ from the value at 0 min.

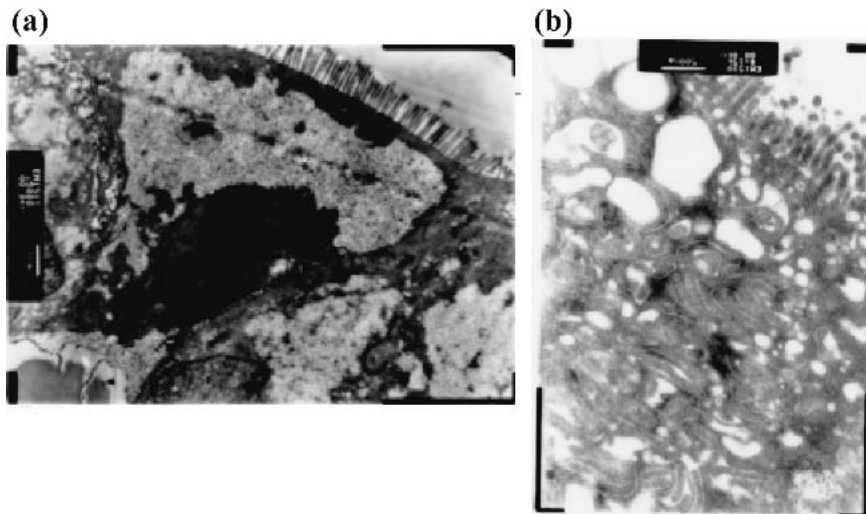


Fig. 6. Transmission electron micrographs of filter-grown Caco-2 monolayer. (a) Control. The inside bar indicates 1 μm . (b) Caco-2 cells exposed to 1.0 mM $[\text{VO}(\text{acac})_2]$ for 60 min. The inside bar indicates 100 nm.

subsequently vanadate oligomers. Therefore, it is conceivable that $[\text{VO}(\text{ma})_2]$ may undergo a faster metabolic process by being oxidized, transformed, and bound to the biogenic molecules in cytoplasm during the monolayer transport. This process may circumvent $[\text{VO}(\text{ma})_2]$ and prevent entrance into the basal compartment and produce a higher level of cellular accumulation. Therefore, high stability of vanadium compounds might be another crucial factor for oral bioavailability.

The toxicity properties are another important issue for the clinical success of vanadium compounds. These compounds have an order of IC_{50} value of $[\text{VO}(\text{acac})_2] < \text{vanadate} < [\text{VO}(\text{ma})_2]$, but the difference among them is not significantly large. Furthermore, the cytotoxicity of vanadium compounds was associated with their capacity of cellular accumulation.

Because the toxicity of transition metal is usually associated with elevated reactive oxygen species (ROS) (20), the

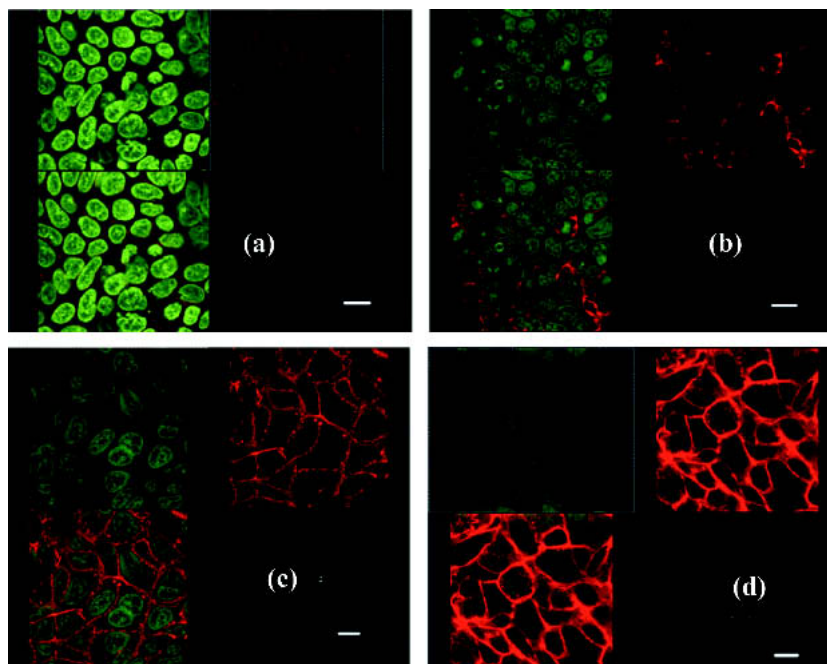


Fig. 7. Fluorescent staining of actin cytoskeleton by rhodamine-phalloidin in intestinal monolayers. (a) control; (b), (c), and (d) indicate Caco-2 cells treated with 1.0 mM of $[\text{VO}(\text{acac})_2]$, $[\text{VO}(\text{ma})_2]$, and NaVO_3 , respectively. Each picture shows the fifth section of a series of 1.1- μm horizontal optical sections of confocal images from the top of apical membrane to the basolateral. The upper left area indicates Hoechst 33258 stained nuclei (green); the upper right area indicates Rhodamine-phalloidin stained F-actin; the lower left area is the overlaid picture. The bars indicate 15 μm .

effects of vanadium compounds on Caco-2 cellular ROS levels were investigated. The experimental results (Fig. 3 and 4) showed that all vanadium compounds resulted in elevation level of $\cdot\text{O}_2^-$, located in the specific area of cytoplasm. This result suggests that vanadium did not induce the generation of ROS by undergoing redox cycling on themselves (21) but by acting most probably on the mitochondria of an organelle, the main resource of the oxygen species (22,23). Because an increased mitochondrial membrane potential ($\Delta\Psi_m$) was observed upon incubation of Caco-2 with the vanadium compounds (data not shown), these results suggest that vanadium might enhance the respiratory metabolism of mitochondria. This action provides a new clue to the currently unclear mechanism of the hypoglycemic effects of vanadium compounds.

The capacity of vanadium compounds to induce ROS was in the same order as cytotoxicity: $[\text{VO}(\text{acac})_2] > \text{vanadate} > [\text{VO}(\text{ma})_2]$, hence, the elevated ROS should contribute to cytotoxicity and at least partially GI stress.

Because the GI stress was of special interest for toxicity of vanadium compounds, effects of the vanadium compounds on fully differentiated Caco-2 monolayer were investigated. As shown in Fig. 7, vanadium compounds resulted in change in the structure of F-actin and microvilli.

The drop of transepithelial electrical resistance (TEER) was the first sign for impairing of integrity of cell monolayer (24). Tight junction was morphologically intact when observed with TEM; however, TEER measurements indicate perturbation of the tight junction. As shown in Fig. 7, treatment of vanadium resulted in condensation of F-actin. As the F-actin filaments are closely associated with tight junctional proteins such as occluding, ZO proteins and cingulin (25), perturbations in cytoskeletal structures may affect the function of tight junction and thus decrease TEER.

One notable change is the destructed microvilli in the apical side. TEM observation (Fig. 6) showed that the microvilli became curled and tangled upon incubation with $[\text{VO}(\text{acac})_2]$. Likewise, the length of the microvilli was shortened, shown by the consecutive sections of Caco-2 monolayer (data not shown). All the above results suggest that F-actin might be one of the major targets, accounting for the GI toxicity of vanadium compounds.

The difference in the perturbation on the F-actin structure of vanadium compounds may partly be attributed to their different transport pathways. In Fig. 7, vanadate, which is mainly transport through the paracellular pathway, produced a heavier condensation of F-actin at the cell-cell contacts. In contrast, $[\text{VO}(\text{acac})_2]$ caused an aggregated F-actin ring primarily at the periphery of cells whose nuclei condensed. This action suggests $[\text{VO}(\text{acac})_2]$ might cause damage of the cells due to high cell accumulation, thus impairing of F-actin later. The change in F-actin structure may be a manifestation of the overall toxicity.

In summary, vanadium compounds ($[\text{VO}(\text{acac})_2]$, $[\text{VO}(\text{ma})_2]$, and vanadate) were shown to pass through the Caco-2 monolayer by a simple diffusion mechanism. The ion channel inhibitor, DIDS, had little effect on their apical to basolateral transport. $[\text{VO}(\text{acac})_2]$ exhibited fairly good permeability. These characteristics of $[\text{VO}(\text{acac})_2]$ may be associated with its high biopotency. $[\text{VO}(\text{ma})_2]$ exhibited a low permeability probably due to metabolic transformation during the absorption process. The toxicity of vanadium com-

plexes on Caco-2 monolayer involved F-actin-related change of tight junction and impairment of microvilli. These changes may be related to the gastrointestinal stress for oral administration. The cytotoxicity of vanadium compounds are also related to elevated intracellular ROS and their cellular accumulation. The study data demonstrate that absorption, metabolism, and toxicity of vanadium compounds may be closely related. More research on design of vanadium compounds with optimal solubility and stability characteristics is indicated.

ACKNOWLEDGMENTS

This research was supported by the National Natural Science Foundation of China (No. 20101001) and by Peking University 985 Preventive Medicine Fund.

REFERENCES

1. N. Cohen, M. Halberstam, P. Shlimovich, C. J. Chang, H. Shamoon, and L. Rossetti. Oral vanadyl sulfate improves hepatic and peripheral insulin sensitivity in patients with non-insulin-dependent diabetes mellitus. *J. Clin. Invest.* **95**:2501–2509 (1995).
2. A. B. Goldfine, D. C. Simonson, F. Folli, M. E. Patti, and C. R. Kahn. In vivo and in vitro studies of vanadate in human and rodent diabetes mellitus. *Mol. Cell. Biochem.* **153**:217–231 (1995).
3. K. H. Thompson, J. H. McNeill, and C. Orvig. Vanadium compounds as insulin mimics. *Chem. Rev.* **99**:2561–2572 (1999).
4. C. Orvig, K. H. Thompson, M. Battell, and J. H. McNeill. Vanadium compounds as insulin mimics. *Met. Ions Biol. Syst.* **31**:575–594 (1995).
5. J. Li, G. Elberg, D. C. Crans, and Y. Shechter. Evidence for the distinct vanadyl(+4)-dependent activating system for manifesting insulin-like effects. *Biochemistry* **35**:8314–8318 (1996).
6. X. G. Yang, K. Wang, J. F. Lu, and D. C. Crans. Membrane transport of vanadium compounds and the interaction with the erythrocyte membrane. *Coord. Chem. Rev.* **237**:103–111 (2003).
7. C. Orvig, K. H. Thompson, B. D. Liboiron, J. H. McNeill, and V. G. Yuen. Biocalculation and in vivo coordination chemistry of vanadium pharmaceuticals. *J. Inorg. Biochem.* **96**:14 (2003).
8. I. J. Hidalgo, T. J. Raub, and R. T. Borcharadt. Characterization of the human colon carcinoma cell line (Caco-2) as a model system for intestinal epithelial permeability. *Gastroenterology* **96**:736–749 (1989).
9. S. Yamashita, T. Furubayashi, M. Kataoka, T. Sakane, H. Sezaki, and H. Tokuda. Optimized conditions for prediction of intestinal drug permeability using Caco-2 cells. *Eur. J. Pharm. Sci.* **10**:195–204 (2000).
10. K. H. Thompson, Y. Tsukada, Z. Xu, M. Battell, J. H. McNeill, and C. Orvig. Influence of chelation and oxidation state on vanadium bioavailability, and their effects on tissue concentrations of zinc, copper, and iron. *Biol. Trace Elem. Res.* **86**:31–44 (2002).
11. J. A. Gordon. Use of vanadate as protein-phosphotyrosine phosphatase inhibitor. *Methods Enzymol.* **201**:477–482 (1991).
12. V. G. Yuen, P. Caravan, L. Gelmini, N. Glover, J. H. McNeill, I. A. Setyawati, Y. Zhou, and C. Orvig. Glucose-lowering properties of vanadium compounds: comparison of coordination complexes with maltol or kojic acid as ligands. *J. Inorg. Biochem.* **68**:109–116 (1997).
13. K. H. Thompson and C. Orvig. Design of vanadium compounds as insulin enhancing agents. *J. Chem. Soc. Dalton Trans.* 2885–2892 (2000).
14. B. A. Reul, S. S. Amin, J. P. Buchet, L. N. Ongemba, D. C. Crans, and S. M. Brichard. Effects of vanadium complexes with organic ligands on glucose metabolism: a comparison study in diabetic rats. *Br. J. Pharmacol.* **126**:467–477 (1999).
15. D. C. Crans. Chemistry and insulin-like properties of vanadium(IV) and vanadium(V) compounds. *J. Inorg. Biochem.* **80**:123–131 (2000).
16. T. Mosmann. Rapid colorimetric assay for cellular growth and survival: application to proliferation and cytotoxicity assays. *J. Immunol. Methods* **65**:55–63 (1983).

17. S. Fraga, B. Sampaio-Maia, M. P. Serrao, and P. Soares-da-Silva. Regulation of apical transporter of L-DOPA in human intestinal Caco-2 cells. *Acta Physiol. Scand.* **175**:103–111 (2002).
18. W. A. Alrefai, S. Tyagi, F. Mansour, S. Saksena, I. Syed, K. Ramaswamy, and P. K. Dudeja. Sulfate and chloride transport in Caco-2 cells: differential regulation by thyroxine and the possible role of DRA gene. *Am. J. Physiol. Gastrointest. Liver Physiol.* **280**:G603–G613 (2001).
19. P. Caravan, L. Gelmini, N. Glover, F. G. Herring, H. Li, J. H. McNeill, S. J. Rettig, I. A. Setyawati, E. Shuter, Y. Sun, A. S. Tracey, V. G. Yuen, and C. Orvig. *J. Am. Chem. Soc.* **117**:12759–12770 (1995).
20. X. G. Yang and X. D. Yang. ADME/Tox approach in inorganic medicinal chemistry. *Prog. Chem.* **14**:273–278 (2002).
21. S. J. Stohs and D. Bagchi. Oxidative mechanisms in the toxicity of metal ions. *Free Radic. Biol. Med.* **18**:321–336 (1995).
22. S. Melov, P. Coskun, M. Patel, R. Tuinstra, B. Cottrell, A. S. Jun, T. H. Zastawny, M. Dizdaroglu, S. I. Goodman, T. T. Huang, H. Miziorko, C. J. Epstein, and D. C. Wallace. Mitochondrial disease in superoxide dismutase 2 mutant mice. *Proc. Natl. Acad. Sci. USA* **96**:846–851 (1999).
23. M. Arai, H. Imai, T. Koumura, M. Yoshida, K. Emoto, M. Umehara, N. Chiba, and Y. Nakagawa. Mitochondrial phospholipid hydroperoxide glutathione peroxidase plays a major role in preventing oxidative injury to cells. *J. Biol. Chem.* **274**:4924–4933 (1999).
24. P. Artursson and C. Magnusson. Epithelial transport of drugs in cell culture. II: effect of extracellular calcium concentration on the paracellular transport of drugs of different lipophilicities across monolayers of intestinal epithelial (Caco-2) cells. *J. Pharm. Sci.* **79**:595–600 (1990).
25. S. A. Peralta, J. M. Mullin, K. A. Knudsen, and C. W. Marano. Tissue remodeling during tumor necrosis factor-induced apoptosis in LLC-PK1 renal epithelial cells. *Am. J. Physiol.* **270**:F869–F879 (1996).
26. X. G. Yang, L. Yuan, K. Wang, and X. D. Yang. Comparison of intestinal absorption of two insulin-mimic vanadyl complexes using Caco-2 monolayers as model system. *Chinese Science Bulletin* **48**:876–881 (2003).